

Selective Oxidation of Linear Alcohols: The Promotional Effect of Water and Inhibiting Effect of Carboxylates over Dilute PdAu Catalysts

Jennifer D. Lee,^{1,†,§,} Amanda Filie,^{2,†} Leigh Wilson,¹ Karin Nguyen,³ Tanya Shirman,^{1,2} Erjia Guan,⁴ Mathilde Luneau,¹ Michael Aizenberg,² Joanna Aizenberg,^{1,2} Robert J. Madix,^{2,‡} Cynthia M. Friend^{1,2,*}*

¹Department of Chemistry and Chemical Biology, Harvard University, Cambridge, MA 02138, USA

²John A. Paulson School of Engineering and Applied Sciences, Harvard University, Cambridge, MA 02138, USA

³Department of Chemistry and Pharmacy, University of Freiburg, Freiburg, Germany

⁴Department of Materials Science and Chemical Engineering, Stony Brook University, Stony Brook, New York 11794, USA.

KEYWORDS: catalysis, bimetallic, dilute alloy, alcohol oxidation, surface poisoning, infrared spectroscopy, palladium, gold

Supporting Information

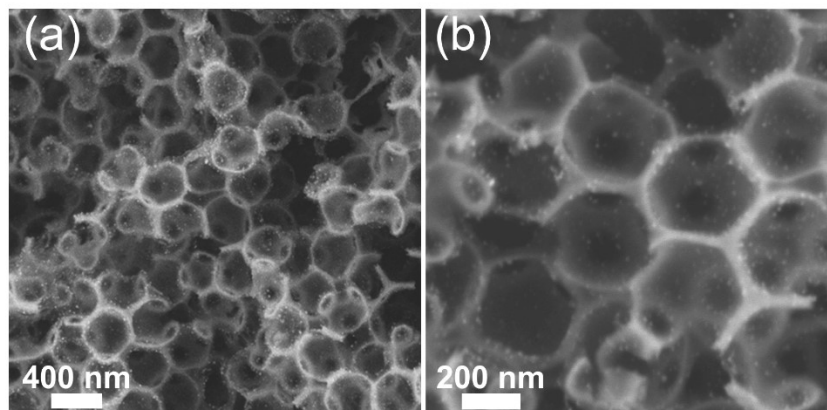


Figure S1. TEM images of Pd₃Au₉₇ RCT-SiO₂ with (a) lower and (b) higher magnifications.

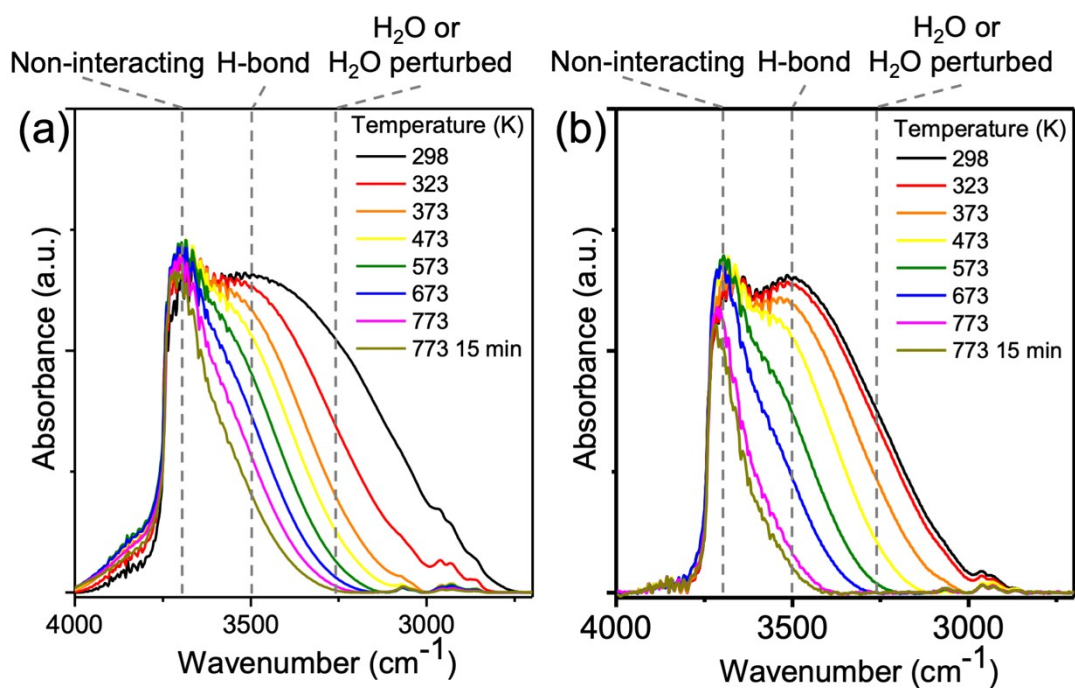


Figure S2. *In-situ* FTIR spectra of (a) RCT-SiO₂ and (b) as-prepared Pd₃Au₉₇ RCT-SiO₂ in the 4000-2700 cm⁻¹ region collected as a function of temperature from 298 to 773 K in O₂. Dashed lines denoted the assignments of silanol groups. Reaction conditions: 100% O₂; flow rate = 20 mL/min.

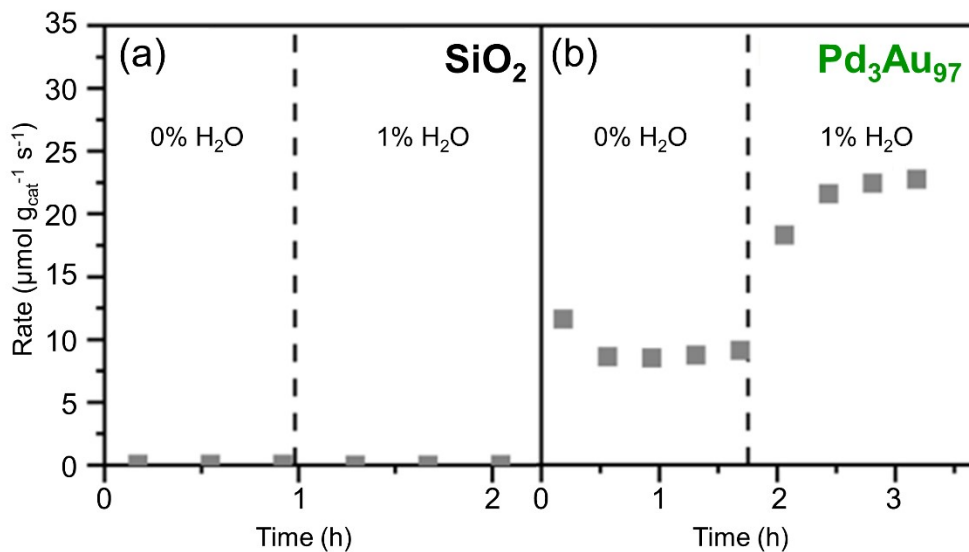


Figure S3. The rate of 1-propanol oxidation over (a) RCT-SiO₂, and (b) Pd₃Au₉₇RCT-SiO₂ in the absence and presence of co-fed 1% H₂O at 423 K. Reaction conditions: 4% 1-propanol, 10% O₂, 0 or 1% H₂O, balanced in He; total flow rate = 50 mL/min; m_{cat} = 40.0 and 10.0 mg for RCT-SiO₂ and Pd₃Au₉₇ RCT-SiO₂, respectively.

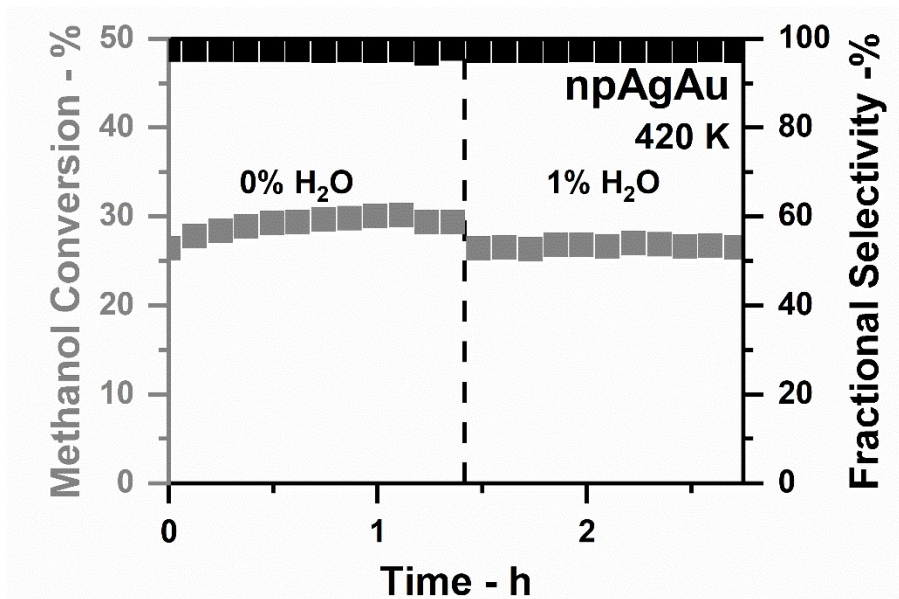


Figure S4. The conversion and selectivity for methanol oxidation reaction over nanoporous AgAu (npAgAu) in the absence and presence of co-fed 1% H₂O at 423 K. Reaction conditions: 10% methanol, 10% O₂, 0 or 1% H₂O, balanced in He; total flow rate = 50 mL/min; $m_{\text{cat}} = 18.0$ mg.

The Au nanoparticle-silica interface was essential to the observed activity of the Au RCT-SiO₂ catalyst for the oxidation of 1-propanol between 423 (Table S1) and 573 K (Table S2). The catalyst-mass normalized rate over the RCT-SiO₂ support for the oxidation of 1-propanol at 423 and 573 K, in the absence and presence of co-fed 1% H₂O, was one order of magnitude smaller than that of either the Au or Pd₃Au₉₇ RCT-SiO₂ catalyst. Although co-feeding 1% H₂O with 1-propanol and O₂ (4% and 10%, respectively) over the Au and Pd₃Au₉₇ RCT-SiO₂ catalysts only promoted conversion at 423 K, it is important to note that H₂O is a byproduct in several reactions of the oxygen-assisted alcohol self-coupling mechanism over Au.^{1,2} Consequently, as 1-propanol is catalyzed by Au in this catalytic cycle, H₂O is generated *in-situ*. Because the FTIR results suggest hydroxyls on the silica remain present on the support up to temperatures as high as 773 K (Figure 1a) and H₂O is generated in substantial quantities over the Pd₃Au₉₇ RCT-SiO₂ catalysts in this temperature range, it is reasonable to assume sufficient water is present in the system at elevated temperatures and interacting with the silica support.

Table S1. The rate and selectivity of 1-propanol oxidation over Au RCT-SiO₂, Pd₃Au₉₇ RCT-SiO₂, and support RCT-SiO₂ in the absence and presence of co-fed 1% H₂O at 423 K. Reaction conditions: 4% 1-propanol, 10% O₂, 0 or 1% H₂O, balanced in He; total flow rate = 50 mL/min; m_{cat} = 10.0, 10.0, and 40.0 mg for Au RCT-SiO₂, Pd₃Au₉₇ RCT-SiO₂, and RCT-SiO₂, respectively.

Catalyst	H ₂ O co-fed (%)	Rate (μmol g _{cat} ⁻¹ s ⁻¹)	Conversion (%)	Propanal	Selectivity (%)		
					Propyl propionate	CO ₂	Alkene +CO ₂
Au	0	4.4 ± 0.3	3.2 ± 0.3	100.0	0.0	0.0	0.0
	1	20.1 ± 0.8	14.7 ± 0.6	83.9	16.1	0.0	0.0
Pd ₃ Au ₉₇	0	8.8 ± 0.3	6.4 ± 0.2	89.5	8.4	0.9	1.3
	1	22.3 ± 0.7	16.3 ± 0.5	82.5	15.9	0.3	1.3
RCT-SiO ₂	0	0.1 ± 0.1	0.2 ± 0.1	100.0	0.0	0.0	0.0
	1	0.0	0.0	0.0	0.0	0.0	0.0

Table S2. The rate of 1-propanol oxidation over Au RCT-SiO₂, Pd₃Au₉₇ RCT-SiO₂, and support RCT-SiO₂ in the absence and presence of co-fed 1% H₂O at 573 K. Reaction conditions: 4% 1-propanol, 10% O₂, 0 or 1% H₂O, balanced in He; total flow rate = 50 mL/min; m_{cat} = 10.0, 10.0, and 40.0 mg for Au RCT-SiO₂, Pd₃Au₉₇ RCT-SiO₂, and RCT-SiO₂, respectively.

Catalyst	H ₂ O co-fed (%)	Rate of 1-propanol oxidation (μmol g _{cat} ⁻¹ s ⁻¹)	Conversion of 1-propanol (%)
Au	0	95.6 ± 1.4	70.1 ± 1.0
	1	93.4 ± 1.2	68.5 ± 0.8
Pd ₃ Au ₉₇	0	110.2 ± 4.4	80.8 ± 3.2
	1	110.1 ± 2.5	80.8 ± 1.8
RCT-SiO ₂	0	2.9 ± 0.1	8.5 ± 0.4
	1	1.9 ± 0.1	5.5 ± 0.1

Table S3. The rate and selectivity of methanol oxidation over Au RCT-SiO₂, Pd₃Au₉₇ RCT-SiO₂, and Pd RCT-SiO₂. Reaction conditions: 10% methanol, 10% O₂, balanced in He; total flow rate = 50 mL/min; m_{cat} = 40.8, 40.5, and 10.0 mg for Au RCT-SiO₂, Pd₃Au₉₇ RCT-SiO₂, and Pd RCT-SiO₂, respectively.

Catalyst	Reaction Temperature (K)	Rate (μmol g _{cat} ⁻¹ s ⁻¹)	Conversion (%)	Selectivity (%)	
				Methyl formate	CO ₂
Au	423	6.7	8.0	97.1	2.9
Pd ₃ Au ₉₇	423	36.2	42.7	89.9	10.1
Pd*	353	96.0	28.0	87.0	13.0

*Note that Pd RCT-SiO₂ was first tested at 423 K but was highly exothermic and required the experiment to be shut down before data could be acquired. The data shown were acquired at 353 K instead; however, due to its exothermic behavior and instability under reaction conditions, sudden increases in CO₂ production were observed over time (“light-off” behavior) and a steady-state conversion was not achievable. The data reported does not consider the “light-off” behavior and instability of Pd RCT-SiO₂.

Table S4. The reaction products of C1 to C4 alcohol oxidation at 423 K over Au and Pd₃Au₉₇ RCT-SiO₂ (corresponding to Figure 2). The alkene products are only observed for Pd₃Au₉₇ RCT-SiO₂ catalysts. Reaction conditions: 4% methanol or 1-propanol, balanced in He; total flow rate = 50 mL/min, m_{cat} = 10.0 mg for both Au and Pd₃Au₉₇ RCT-SiO₂.

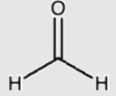
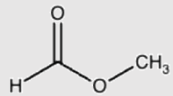
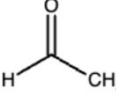
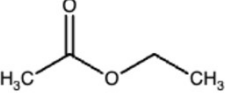
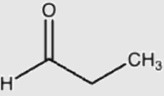
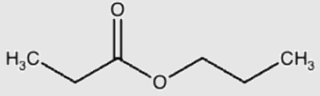
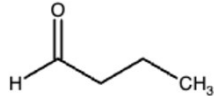
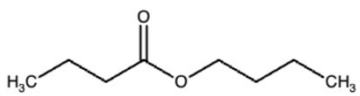
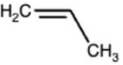
Reactant	Reaction Products			
	Aldehyde	Combustion	Coupling	Alkene
Methanol	 Formaldehyde	CO ₂	 Methyl Formate	ND
Ethanol	 Acetaldehyde	CO ₂	 Ethyl Acetate	ND
1-Propanol	 Propanal	CO ₂	 Propyl Propionate	H ₂ C=CH ₂ Ethylene
1-Butanol	 Butanal	CO ₂	 Butyl Butyrate	 Propylene

Table S5. The rate and selectivity of alcohol oxidation (C1-C4) over Au RCT-SiO₂ and Pd₃Au₉₇ RCT-SiO₂ at 423 K. Reaction conditions: 4% alcohol, 10% O₂, balanced in He; total flow rate = 50 mL/min; m_{cat} = 40.0 and 40.5 mg for Au RCT-SiO₂ and Pd₃Au₉₇ RCT-SiO₂, respectively.

Catalyst	Alcohol	Rate ($\mu\text{mol g}_{\text{cat}}^{-1}$ s^{-1})	Conversion (%)	Selectivity (%)			
				Aldehyde	Coupling	Combustion	Alkene +CO ₂
Au	Methanol	9.5 ± 0.1	27.9 ± 0.3	N/A	94.4 ± 1.0	5.6 ± 0.1	N/A
	Ethanol	5.0 ± 0.1	14.8 ± 0.1	83.3 ± 0.1	16.7 ± 2.0	N/A	N/A
	1-Propanol	9.6 ± 0.4	28.1 ± 1.0	80.4 ± 4.0	19.6 ± 2.1	N/A	N/A
	1-Butanol	8.6 ± 0.2	25.4 ± 0.5	100.0 ± 0.1	N/A	N/A	N/A
Pd ₃ Au ₉₇	Methanol	33.0 ± 0.1	98.1 ± 0.2	N/A	62.7 ± 0.8	37.3 ± 0.8	N/A
	Ethanol	6.2 ± 0.2	18.4 ± 0.5	76.5 ± 1.0	21.1 ± 0.9	2.4 ± 0.1	N/A
	1-Propanol	9.1 ± 1.0	27.0 ± 2.9	79.0 ± 1.5	17.9 ± 1.3	0.7 ± 0.1	2.3 ± 0.2
	1-Butanol	7.2 ± 0.3	21.5 ± 0.8	93.2 ± 0.2	N/A	0.3 ± 0.1	6.5 ± 0.1

Table S6. The rate of methanol or 1-propanol conversion over Au and Pd₃Au₉₇ RCT-SiO₂ catalysts under non-oxidative conditions. Reaction conditions: 4% methanol or 1-propanol, balanced in He; total flow rate = 50 mL;min, m_{cat} = 10.0 mg for both Au and Pd₃Au₉₇ RCT-SiO₂.

Catalyst	Temperature (K)	Alcohol	Rate ($\mu\text{mol g}_{\text{cat}}^{-1} \text{s}^{-1}$)
Pd ₃ Au ₉₇ RCT-SiO ₂	423	Methanol	0.4±0.1
	423	1-Propanol	0.3±0.1
	573	Methanol	1.7±0.6
	573	1-Propanol	3.5±0.7
Au RCT-SiO ₂	423	Methanol	0.2±0.2
	423	1-Propanol	0.4±0.1
	573	Methanol	0.6±0.6
	573	1-Propanol	3.4±0.8

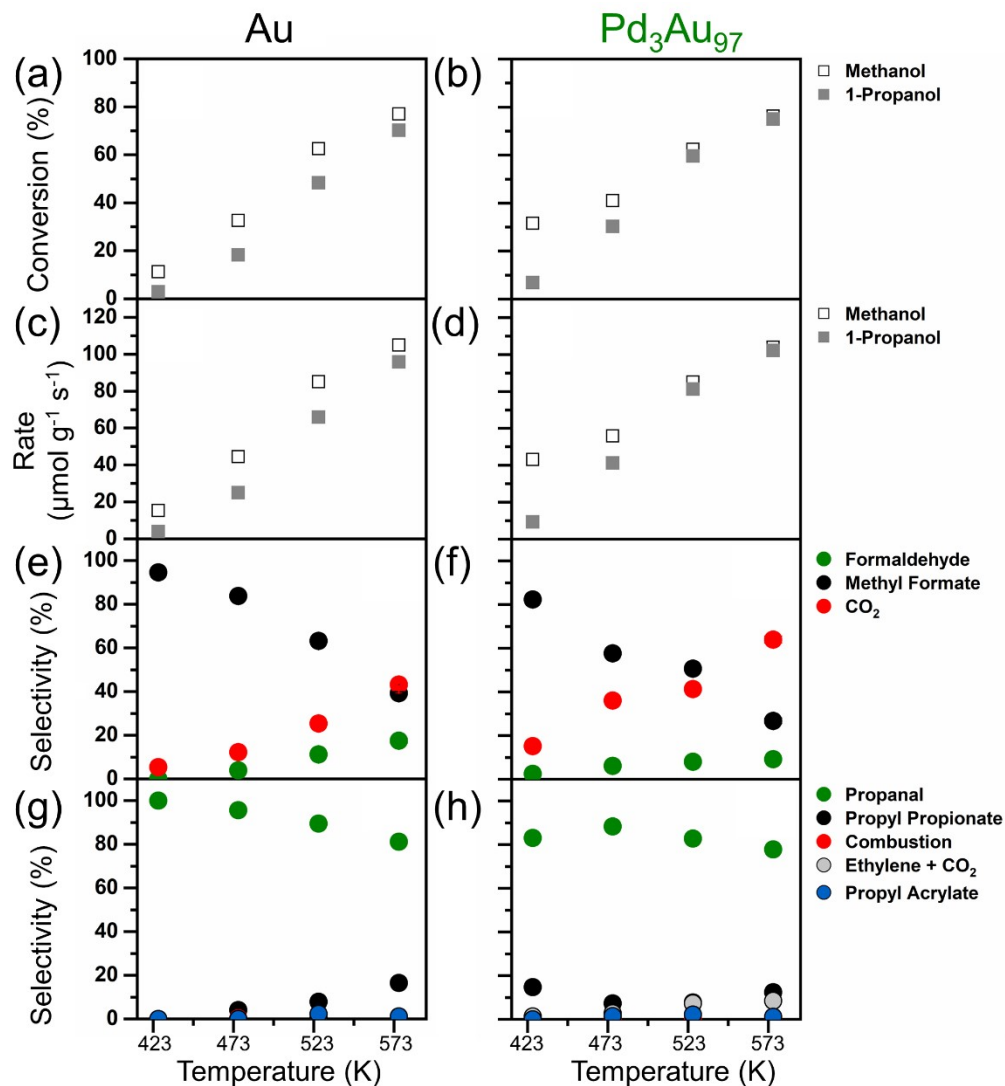


Figure S5. The conversion of methanol and 1-propanol and the rate of oxidation over the (a,c) Au and (b,d) Pd₃Au₉₇ RCT-SiO₂ catalysts, and the corresponding selectivity over (e,g) Au and (f,h) Pd₃Au₉₇ RCT-SiO₂ catalysts. Reaction conditions: 423 K ≤ Temperature ≤ 573 K, 4% methanol or 1-propanol, 10% O₂, balanced in He; total flow rate = 50 mL/min; m_{cat} = 10.0 mg for both Au and Pd₃Au₉₇ RCT-SiO₂.

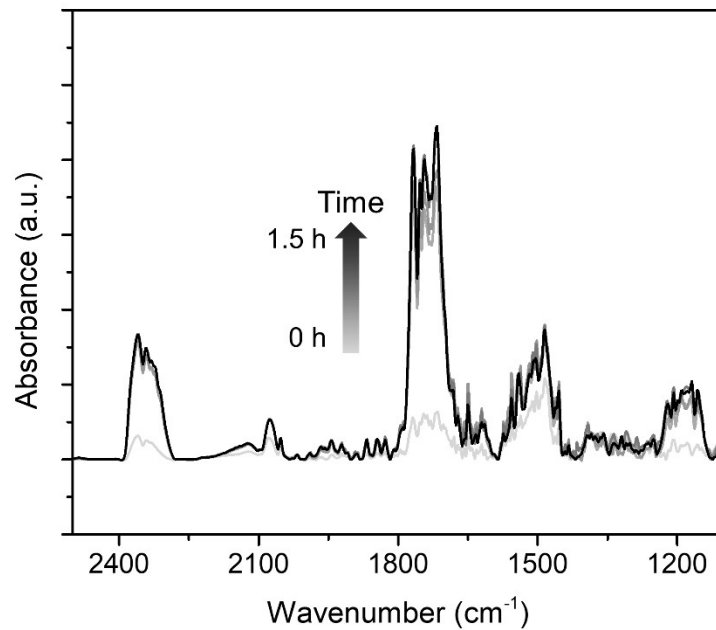


Figure S6. *In-situ* FTIR spectra in the 2500-1100 cm⁻¹ region collected as a function of time (0-1.5 h) during the oxidation of methanol over Pd₃Au₉₇ RCT-SiO₂ at 423 K. Reaction conditions: 4% alcohol and 10% O₂, balanced in He; total flow rate = 20 mL/min.

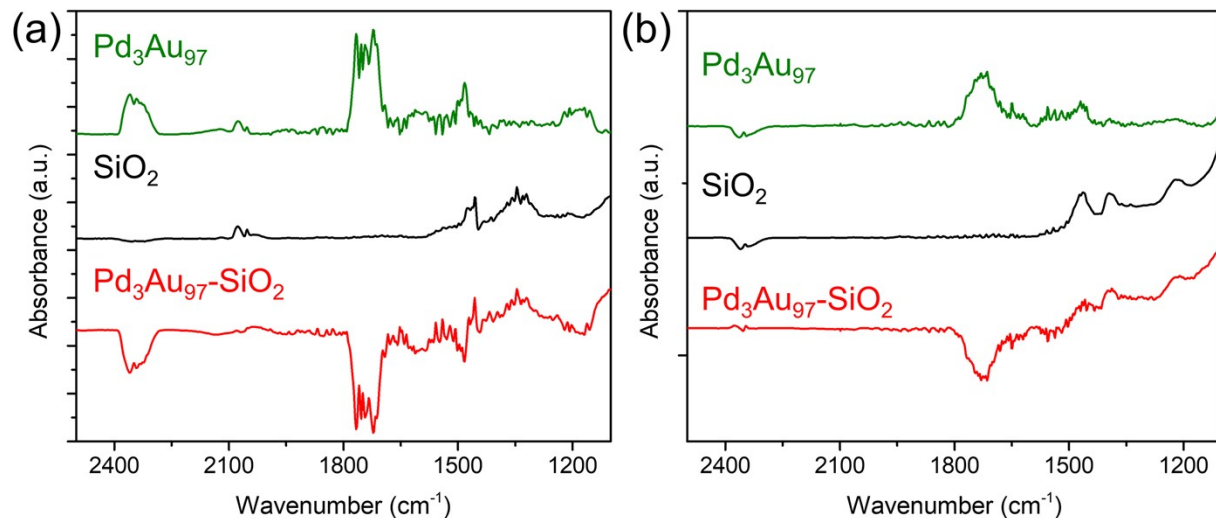


Figure S7. *In-situ* FTIR spectra in the 2500-1100 cm⁻¹ region of the difference (red) between steady-state spectra of species on Pd₃Au₉₇ RCT-SiO₂ (green) and SiO₂ (black) formed during the oxidation of (a) methanol and (b) 1-propanol for 90 min. Downward features in the difference spectra (red) are contributions from the products. Reaction conditions: temperature = 423 K; 4% alcohol and 10% O₂, balanced in He, total flow rate = 20 mL/min.

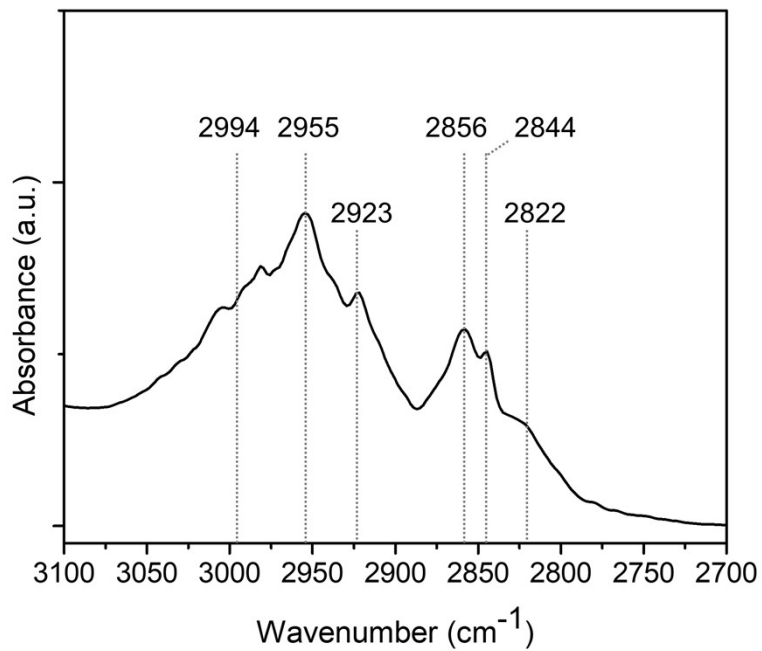


Figure S8. *In-situ* FTIR spectra in the C-H region (2700-3100 cm⁻¹) of Pd₃Au_{0.7} RCT-SiO₂ under steady-state methanol oxidation reaction conditions. Dashed lines denoted IR peaks of interest. Reaction conditions: temperature = 423 K; 4% alcohol and 10% O₂, balanced in He, total flow rate = 20 mL/min.

The accumulation of surface species on Pd₃Au₉₇ RCT-SiO₂ under 1-propanol oxidation reaction was further confirmed using the integrated area in spectral region characteristic for C=O and C-O stretches (1900-1100 cm⁻¹) collected as a function of time (Figure S9). The integrated area of *in-situ* FTIR spectra collected after methanol oxidation starts to decrease after purging in He at 423 K and reaches a minimum level after 2 h (Figure S9a), which indicates the desorption of both gas phase and surface-bound species. In contrast, purging in He after 1-propanol oxidation showed a close to zero decrease in the integrated area (Figure S9b), indicative of surface-bound species present even after purging in He for 2 h. These changes in the integrated area support the formation of strongly bound surface species poisoning Pd active sites under 1-propanol oxidation conditions, which resulted in minimal promotional effect of Pd₃Au₉₇ RCT-SiO₂ towards C₂-C₄ alcohols oxidation as observed in the reactor studies. *In-situ* FTIR spectra of alcohol oxidation over SiO₂ were also collected as a control to eliminate the contribution from molecules adsorbed on the support alone (Figure S9 black). Both integrated absorbance in the 1900-1100 cm⁻¹ region of *in-situ* FTIR spectra collected after methanol and 1-propanol oxidation showed continuous decrease in the integrated area after purging in He. This suggests the removal of gas species as no reaction will happen on the support SiO₂ itself.

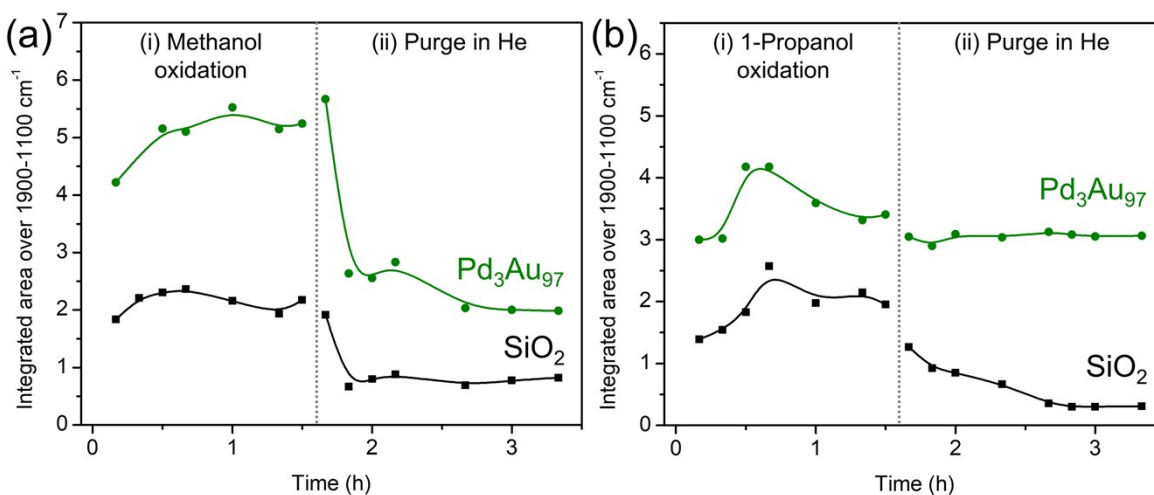


Figure S9. The integrated absorbance in the 1900-1100 cm⁻¹ region of *in-situ* FTIR spectra collected as a function of time during (i) the oxidation of (a) methanol and (b) 1-propanol over Pd₃Au₉₇ RCT-SiO₂ (green) and SiO₂ support (black) for 1.5 h followed by (ii) purging in He for 2 h. Reaction conditions: temperature = 423 K; 4% alcohol and 10% O₂, balanced in He, total flow rate = 20 mL/min.

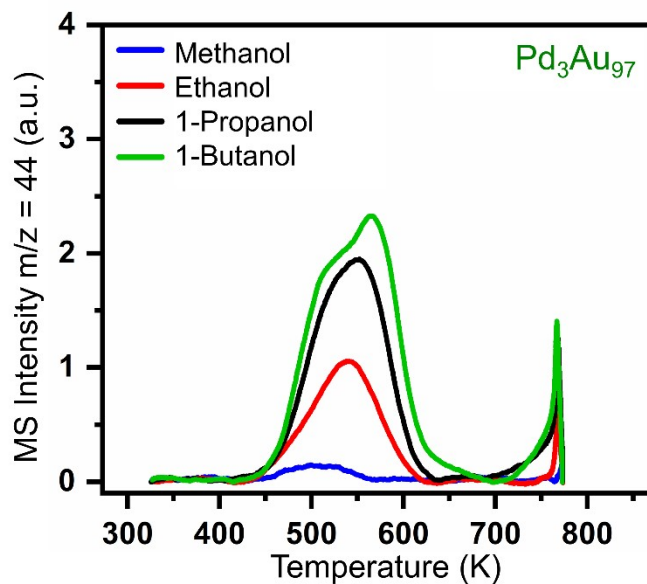


Figure S10. The production of CO₂ during the temperature programmed oxidation (TPO) between 298-773 K of used Pd₃Au₉₇ RCT-SiO₂ catalysts after the oxidation of alcohols (C1-C4) for ~2 h at 423 K. TPO conditions: ramp rate = 10 K/min; 10% O₂ balanced in He; total flow rate = 20 mL/min; m_{cat} = 40.5 mg.

Table S7. Temperature-programmed desorption temperature of carboxylates reported on Au(111) or Au(110) single crystal and the CO₂ formation peak temperature during the TPO of post-reaction Pd₃Au₉₇ RCT-SiO₂ catalysts (corresponding to Figure S10).

Au(111) or Au(110) single crystal			Pd₃Au₉₇ RCT-SiO₂	
Carboxylate	Temperature (K)		Alcohol	Temperature (K)
	Limited O	Excess O		
Formate ³	350	--	Methanol	493
Acetate ⁴	530	425	Ethanol	548
Propionate ⁵	555	410, 465	1-Propanol	553
Butyrate ⁶	530	--	1-Butanol	492, 563

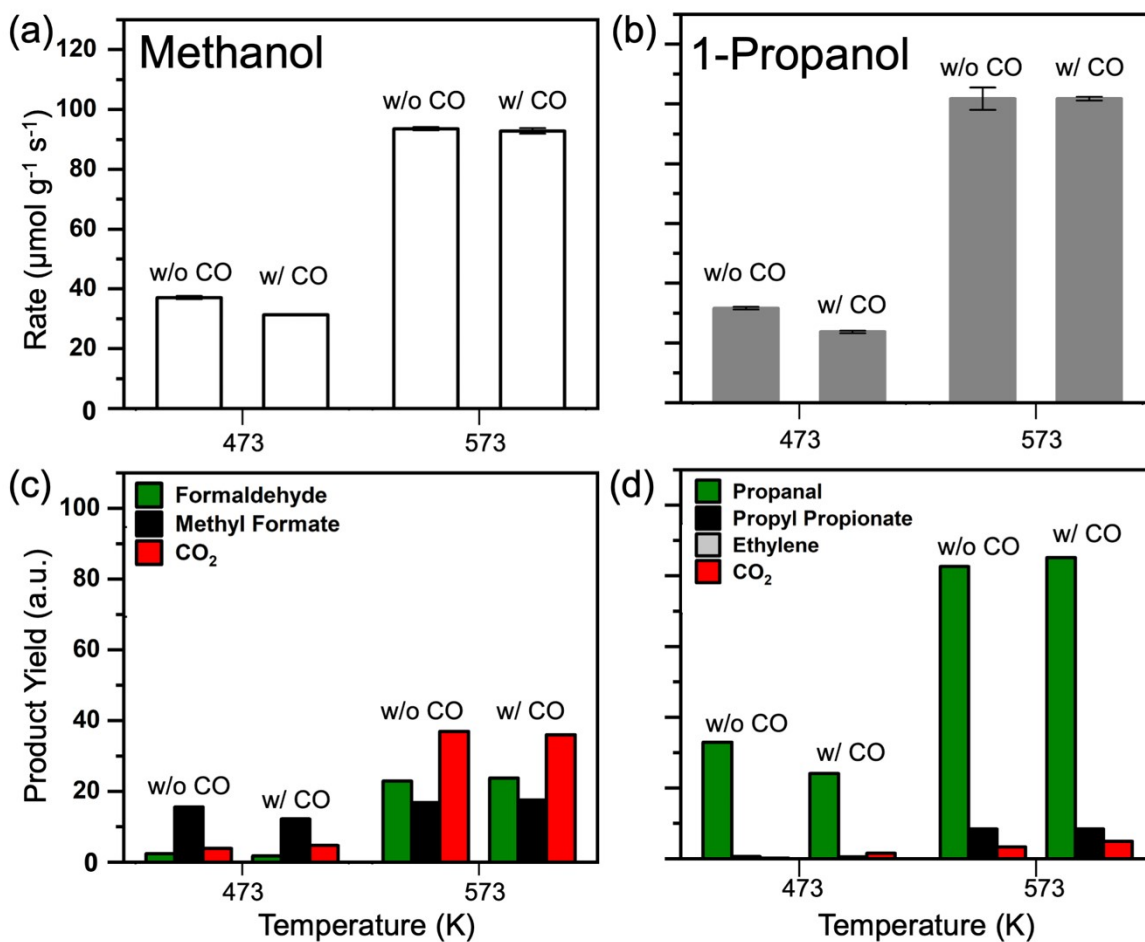


Figure S11. The rate of (a) methanol and (b) 1-propanol oxidation in the absence (w/o CO) and presence (w/ CO) of co-fed 2% CO at 473 K and 573 K over Au RCT-SiO₂, and the corresponding yield of products during (c) methanol and (d) 1-propanol oxidation. Reaction conditions: 4% 1-propanol, 10% O₂, 0 or 2% CO, balanced in He; total flow rate = 50 mL/min; $m_{\text{cat}} = 10.0$ mg.

Equations for conversion of alcohol and selectivity:

The previously described method for calculating the conversion of alcohol using reaction stoichiometry and quantifying products using a combined gas chromatograph-mass spectrometer^{7,8} was used. A more detailed summary is provided here. The relative amount of molecule i (n_i) is given by eq 1:

$$n_i = \frac{A_i}{\sigma_i} \quad (1)$$

where A_i is the area under the total ion current signal forming a peak generated by molecule i (arbitrary units), and σ_i is the total ionization cross section of molecule i (\AA^2). The total ionization cross-section for all species is summarized in Table S8.

Table S8. Total ionization cross-section for molecules observed in the oxidation of alcohols

molecule	σ	ref.	molecule	σ	ref.
CO ₂	3.5	9	Propanal	9.7	10
Formaldehyde ^a	4.1	10,11	1-Propanol	10.15	10
Methanol	5.01	12	Propyl Propionate	18.36	12
Methyl Formate	7.68	12	Propyl Acrylate	16	10
Acetaldehyde	6.7	10	Propylene	8.82	13
Ethyl Acetate	13.8	10	Butanal	12.4	10
Ethylene	5.39	14	1-Butanol	12.85	10

^aEstimated ionization cross-section using two sources.

The amount of carbon coming into the reactor was assumed to be the same as that coming out of the reactor, making eq 2 true.

$$n_{carbon} = N_{carbon, alcohol} \cdot n_{alcohol in} = \sum N_{carbon,i} \cdot n_i \quad (2)$$

where $N_{carbon,i}$ is the number of carbons in molecule i ,

n_i is the relative quantity of molecule i detected in the mass spectrometer,

i is the index number of all reactants and products in the reactor effluent.

The general expression for conversion of an alcohol is given by eq 3.

$$X_{alcohol} = \frac{\sum_p N_{carbon,p} \cdot n_p}{\sum_i N_{carbon,i} \cdot n_i} \cdot 100\% \quad (3)$$

where p is the index number of the products in the reactor effluent.

The rate of alcohol consumed (eq 4) is readily calculated assuming the ideal gas law, using the reaction conditions and normalizing by the mass of catalyst in the bed.

$$Rate = \frac{X_{alcohol} \cdot P \cdot x_{alcohol\ inlet} \cdot F_{total\ inlet}}{R \cdot T \cdot m_{cat}} \cdot C_{const} \quad (4)$$

where $X_{alcohol}$ is the conversion of alcohol (dimensionless),

P is standard, atmospheric pressure (101,325 Pa),

$x_{alcohol\ inlet}$ is the inlet concentration of alcohol,

$F_{total\ inlet}$ is the total inlet flow rate (50 mL/min),

R is the ideal gas constant (8.314 J/(mol*K)),

T is the standard temperature (298 K),

m_{cat} is the mass of catalyst (g), and

C_{const} is the product of constants to convert the $Rate$ to units of $\mu\text{mol g}_{cat}^{-1} \text{s}^{-1}$.

Because at least an equimolar amount of CO₂ to the alkene product formed, this stoichiometry was accounted for when calculating the fractional selectivity associated with the oxidation of 1-propanol or 1-butanol. The amount of CO₂ associated with the combustion pathway (eq 5) is given by the different of the total amount of CO₂ formed and the stoichiometric amount of CO₂ formed from the alkene formed.

$$n'_{CO_2} = n_{CO_2} - \frac{1 \text{ mol } CO_2}{1 \text{ mol alkene}} \cdot n_{alkene} \quad (5)$$

The selectivity to methyl formate (eq 6), ethyl acetate (eq 7), propyl propionate (eq 8) and butanal (eq 9) are given explicitly to show the assumptions made regarding reaction stoichiometry for the oxidation of methanol, ethanol, 1-propanol, and 1-butanol. Note the units of the coefficients are not explicitly indicated in the equations so the variables are clear. The units for the coefficients are derived from the stoichiometric ratio between the alcohol and the product indicated in the variable n_p , where the subscript p is a carbon-containing product. Thus, all coefficients have units of moles of alcohol divided by moles of the product indicated.

$$S_{Methyl \ formate} = \frac{2 \cdot n_{Methyl \ formate}}{(2 \cdot n_{Methyl \ formate} + 1 \cdot n_{Formaldehyde} + 1 \cdot n_{CO_2})} \quad (6)$$

$$S_{Ethyl \ acetate} = \frac{2 \cdot n_{Ethyl \ acetate}}{(2 \cdot n_{Ethyl \ acetate} + 1 \cdot n_{Acetaldehyde} + 1/2 \cdot n_{CO_2})} \quad (7)$$

$$S_{Propyl \ propionate} = \frac{2 \cdot n_{Propyl \ propionate}}{(2 \cdot n_{Propyl \ propionate} + 2 \cdot n_{Propyl \ acrylate} + 1 \cdot n_{Pr}} \quad (8)$$

$$S_{\text{Butanal}} = \frac{1 \cdot n_{\text{Butanal}}}{\left(1 \cdot n_{\text{Butanal}} + \frac{1}{4} \cdot n'_{\text{CO}_2} + 1 \cdot n_{\text{Propylene}}\right)} \quad (9)$$

References

- 1 C. Reece, E. A. Redekop, S. Karakalos, C. M. Friend and R. J. Madix, *Nat Catal*, 2018, **1**, 852–859.
- 2 B. Xu, X. Liu, J. Haubrich, R. J. Madix and C. M. Friend, *Angewandte Chemie International Edition*, 2009, **48**, 4206–4209.
- 3 C. R. O'Connor, F. Hiebel, W. Chen, E. Kaxiras, R. J. Madix and C. M. Friend, *Chem Sci*, 2018, **9**, 3759–3766.
- 4 C. G. F. Siler, T. Cremer, J. C. F. Rodriguez-Reyes, C. M. Friend and R. J. Madix, *ACS Catal*, 2014, **4**, 3281–3288.
- 5 C. R. O'Connor, Harvard University, 2020.
- 6 J. C. F. Rodriguez-Reyes, C. G. F. Siler, W. Liu, A. Tkatchenko, C. M. Friend and R. J. Madix, *J Am Chem Soc*, 2014, **136**, 13333–13340.
- 7 T. Shirman, J. Lattimer, M. Luneau, E. Shirman, C. Reece, M. Aizenberg, R. J. Madix, J. Aizenberg and C. M. Friend, *Chemistry - A European Journal*, 2018, **24**, 1743.
- 8 L.-C. Wang, K. J. Stowers, B. Zugic, M. M. Biener, J. Biener, C. M. Friend and R. J. Madix, *Catal. Sci. Technol.*, 2015, **5**, 1299–1306.
- 9 J. E. Hudson, C. Vallance and P. W. Harland, *Journal of Physics B: Atomic, Molecular and Optical Physics*, 2003, **37**, 445–455.
- 10 J. N. Bull, P. W. Harland and C. Vallance, 2012, 767–777.
- 11 Y. Xu, W. Chen, E. Kaxiras, C. M. Friend and R. J. Madix, *J Phys Chem B*, 2018, **122**, 555–560.
- 12 J. E. Hudson, Z. F. Weng, C. Vallance and P. W. Harland, *Int J Mass Spectrom*, 2006, **248**, 42–46.

- 13 H. Nishimura and H. Tawara, *J. Phys. B At. Mol. Opt. Phys.*, 1994, **27**, 2063–2074.
- 14 C. Tian and C. R. Vidal, *Chem Phys Lett*, 1998, **288**, 499–503.